The *BaramicinA* gene is required at several steps of the host defense against *Enterococcus faecalis* and *Metarhizium robertsii* in a septic wound infection model in *Drosophila melanogaster*

Jianqiong Huang[1], Yanyan Lou[1], Jiyong Liu[1], Philippe Bulet[5,6], Renjie Jiao[1], Jules A. Hoffmann[1,2,3,4], Samuel Liégeois[1,2,3], Zi Li[1], and Dominique Ferrandon[1, 2,3]

1) Sino-French Hoffmann Institute, Guangzhou Medical University ,Guangzhou, China GMU
2) Université de Strasbourg, Strasbourg, France
3) M3I, UPR 9022 du CNRS, Strasbourg, France
4) USIAS, Institute for Advanced Study of the Université de Strasbourg, Strasbourg, France
5) CR Université Grenoble Alpes, Institute for Advanced Biosciences, Inserm U1209, CNRS UMR 5309, Grenoble, France
6) Platform BioPark Archamps, Archamps, France

Abstract

The host defense against several Gram-positive bacterial and fungal infections is mostly mediated by the Toll pathway in *Drosophila*, which regulates the expression of multiple genes including effectors of the innate immune response. One such potential effector is IMPPP/BaraA, a precursor protein that is processed at furin cleavage sites into an armamentarium of small DIM peptides that display a high degree of sequence similarity. We report here the generation of multiple mutants affecting this gene. Our phenotypic analysis revealed a specific sensitivity to pathogens belonging to distinct kingdoms, the Gram-positive bacterium *Enterococcus faecalis* and the entomopathogenic fungus *Metarhizium anisopliae*, only in septic injury models of infection. Unexpectedly, we failed to reveal a consistently increased microbial burden in the mutant flies infected with either of these microorganisms, opening the possibility for a role of *BaraA* in resilience rather than in resistance, which we were however unable to confirm. We also found that some BaraA-derived DIM peptides display an antimicrobial activity at millimolar concentrations *in vitro.* BaraA is additionally required for an efficient cleavage of pro-phenol oxidase into an active enzyme. BaraA is also involved in the cellular host defense, but through distinct mechanisms: it needs to be expressed in hemocytes for an efficient response solely to *E. faecalis* infection whereas it is required for the uptake by plasmatocytes of *M. robertsii* conidia. We propose a model whereby BaraA secreted by hemocytes may act at a very short range and protect host tissues or organs targeted specifically by *E. faecalis*. This study thus reveals an unexpected functional complexity of a potential effector of the Toll pathway in the host defense against specific infections.

Introduction

Multicellular organisms have evolved in a world dominated by microbes and it is likely that the common ancestor to animals had developed a primeval immune system. Animals, while being constantly exposed to microbes, are infected only occasionally by pathogens. As an immune response is often energetically costly and may also be detrimental to the host, evolution has selected inducible immune responses that are triggered upon infection. Thus, one approach to study immune systems is to focus on genes induced when microbes are in direct contact with the host barrier epithelia or when the internal milieu is invaded.

Drosophila melanogaster constitutes a powerful model to understand the principles of innate immunity that are often useful to comprehend our own host defenses. In addition to its sophisticated genetics, large numbers of insects are available to perform survival to infection studies. An added dimension is that this genetic model organism can also be studied in the wild thanks to the approaches of population genetics; also, evolutionary insights are provided by the sequencing of the genomes of more than 20 Drosophila species as well as those of other Dipterans (Chapman et al., 2019; Duxbury et al., 2019; Hanson et al., 2019b; Lazzaro, 2008; Longdon et al., 2015; McKean et al., 2008; Sackton et al., 2007). *Drosophila* immunity has now been studied for thirty years. Besides the cellular immune system found in most animals and the arthropod-specific melanization host defense mediated by the activation of the prophenol oxidase enzyme, a major focus of investigations has been the systemic humoral immune response mediated by the NF-kappaB signaling pathways Immune deficiency (IMD) and Toll (Buchon et al., 2014; Ferrandon et al., 2007; Lemaitre and Hoffmann, 2007). While the former plays a preponderant role in the host defense against Gram-negative bacterial infections, the latter is essentially activated by Gram-positive bacterial and fungal infections and is required in the host defense against such infections. Of note, the Toll pathway is also

activated by highly pathogenic Gram-negative bacteria such as *Pseudomonas aeruginosa* that cause an uncontrolled bacteremia (Lau et al., 2003; Limmer et al., 2011). Drosomycin is an antimicrobial peptide (AMP) active against some filamentous fungi and that was initially identified thanks to its strong induction in the hemolymph of immune-stimulated flies (Fehlbaum et al., 1995). This gene is often used as a convenient read-out of Toll pathway activation. However, microarrays and subsequent RNAseq studies have revealed that the Toll pathway regulates the expression of more than 250 genes after immune challenges, the function of many of which remains to be characterized (Boutros et al., 2002; De Gregorio et al., 2002; De Gregorio et al., 2001; Irving et al., 2001; Troha et al., 2018). Up-regulated genes include known AMPs such as the antifungal peptide Metchnikowin. Thus, some of these genes may correspond to effectors of the immune response. Indeed, the molecules that are active against Gram-positive bacteria remain to be identified. While the one gene encoding an AMP described to be active against Gram-positive bacteria *in vitro*, *Defensin*, is induced jointly by the Toll and IMD pathways, it is unlikely to be a major effector: IMD pathway mutant flies do not induce *Defensin* expression yet are resistant to Gram-positive bacterial infections such as *Staphylococcus aureus* or *Enterococcus faecalis* (Rutschmann et al., 2000). Other induced genes may correspond to genes involved in the positive or negative regulation of the Toll pathway, for instance of serpin protease inhibitors that negatively regulate the proteolytic cascades that mature the Spätzle cytokine into an active Toll ligand (De Gregorio et al., 2002; Ligoxygakis et al., 2002).

The host defense against infections is not limited to resistance, that is, the production of effectors that kill or neutralize pathogens. It also encompasses a second dimension, known as resilience or tolerance, which regroups the physiological mechanisms that allow the host to endure or repair damages inflicted by the virulence factors of pathogens or by the host's own immune response (Ferrandon, 2013; Medzhitov et al., 2012; Soares et al., 2017). For instance,

the Immune Responsive Catalase IRC is induced by an immune challenge in a Toll-dependent manner and might be required in regulating a ROS response triggered by injury (Capilla et al., 2017; Nam et al., 2012). This however remains to be formally demonstrated in the framework of the systemic humoral immune response. A gene upregulated by septic or sterile injury is *Materazzi* and has been shown to be required in Malpighian tubules to remove from the hemolymph oxidized lipids generated upon injury (Li et al., 2020). The CrebA gene has been shown to be required in the host defense against bacterial infections, often displaying a mild susceptibility phenotype. Monitoring the bacterial burden at several time points during infection failed to reveal any significant difference between wild-type and mutant flies. However, mutant flies were killed by a much lower dose of bacteria than wild-type or Toll pathway mutant flies, as determined by the bacterial number upon death (BLUD) parameter (Duneau et al., 2017). Indeed, CrebA is a gene that regulates the expression of genes involved in secretion. In its absence, flies likely succumb to endoplasmic reticulum stress taking place in the fat body (Troha et al., 2018). Thus, parameters useful to discriminate between genes involved in resistance and genes involved in resilience against bacterial infections are respectively the bacterial load during infection and the BLUD. Of note, these parameters are not absolute in that some pathogens kill their host in the absence of proliferation, *e.g.,* by toxins (Xu *et al*., in preparation) and it is not clear whether mutations such as *materazzi* would alter the BLUD.

While transcriptomics is a powerful approach to identify genes regulated by the Toll and IMD pathways, an interesting counterpoint is provided by proteomics approaches that focus on the protein level. Besides techniques such as 2D gel electrophoresis or liquid chromatography-mass spectrometry that allow to compare large proteins induced or not in Drosophila by an immune challenge, matrix-assisted laser desorption/ionization time-of-flight mass spectrometry (MALDI-TOF) revolutionized the biochemical approach by allowing to detect the induction of peptides of limited sizes (up to 15 kD) in the hemolymph collected from single flies. It led to

the identification of a series of peptides induced by immune challenges, referred to as Drosophila induced immune molecules (DIMs) (Uttenweiler-Joseph et al., 1998). Some of the induced peaks correspond to previously identified AMPs such as Drosocin, Metchnikowin, prodomain of AttacinD, or Drosomycin (Levy et al., 2004a; Levy et al., 2004b).

DIM4 and DIM14 are related peptides with a somewhat overlapping but not entirely redundant function in the host defense against some filamentous fungi and may be involved in resistance as the flies deleted for these two genes display a modestly increased fungal burden (Cohen et al., 2020).

Another category of DIMs shares a conserved Bomanin domain. The Bomanin family comprises three categories of proteins: short BomS corresponding to the Bomanin domain, intermediate BomT proteins with a tail after the Bomanin domain, and bicipital BomBc ones with two Bomanin domains. Ten Bomanin genes are found at the 55C locus; strikingly, the deletion of the locus presents a phenotype as strong as Toll pathway mutants after infection with Gram-positive bacteria such as *E. faecalis*, filamentous fungi, and pathogenic yeasts (Clemmons et al., 2015). This discovery suggests that Bomanins are major mediators of the Toll pathway action. However, no antimicrobial activity has been detected *in vitro* so far, even though the bacterial titer increases in *E. faecalis*-challenged 55C flies as compared to wild-type, suggesting a role for this locus in resistance to this pathogen. Further studies on BomS peptides showed that they are required for the fungicidal activity of hemolymph on *Candida glabrata* (Lindsay et al., 2018). The concentration rather than the exact nature of the BomS peptide appears to be relevant in the host defense against *C. glabrata.* Of note, the presence of BomS but not BomBc peptides in the hemolymph requires the expression of a Toll-regulated protein named Bombardier (Lin et al., 2019). Interestingly, this protein appears to be involved both in resistance, through the stabilization of BomS peptides in the hemolymph and in resilience, because of a detrimental effect of BomS peptides in its absence. Finally, flies for which the

expression of *BomBc1* is attenuated by RNAi have been reported to be sensitive to *E. faecalis* infection (Chapman et al., 2020).

An unusual situation concerns the related peptides DIM5, DIM6, DIM8, DIM10, DIM12, and DIM13 which are highly related and actually derived from the processing of large precursor protein named IMPPP, which also contains the DIM24 peptide at its N-terminal domain (Fig. 1A-B). This situation is akin to the formation of neuropeptides that are also found initially in large precursor proteins. The knockdown of its expression did not reveal a role in host defense against infections nor a role in phagocytosis (Levy et al., 2004a).

Here, we have extensively characterized the IMPPP locus, which is duplicated in some *D. melanogaster* lines, and report a specific requirement for IMPPP in host defense against two specific infections, the Gram-positive bacterium *E. faecalis* and the entomopathogenic fungus *Metarhizium robertsii* in a septic injury but not "natural" infection through the cuticle paradigm. Even though we find that *IMPPP* is needed for a full activation of melanization and is also required for the uptake of injected *M. robertsii* conidia by plasmatocytes, we have not found a clear-cut role for this gene in either resistance or resilience.

Given the peculiar genomic organization of the gene as well as the presence of multiple highly related peptides derived from a single precursor protein, we have agreed to renaming the gene *BaraA*, an allusion to the Japanese expression *Bara Bara*, which refers among other meanings to objects or entities broken apart and scattered.

Results

Generation of mutants affecting the expression of the BaraA gene

One unexpected feature of the *BaraA* locus in the genome sequence of the *Drosophila melanogaster* genome is that it appears to be perfectly duplicated in tandem along with its neighboring gene over a region of 4727 nucleotides with just a unique six-nucleotide sequence forming the junction between the two repeated sequences (Fig. S1A). The two genes named *CG18279* and *CG33470* encode the *BaraA* gene, whereas the neighboring genes are *CG18278* and *CG30059*. Because such a perfect duplication is likely to be unstable, we designed primers to test whether the duplication was present in a variety of wild-type lines (Fig. S1B). We found that there was only one copy in most tested lines except w^{1118} and the *BaraA* Knock down 2 RNAi line.

BaraA gene expression is hardly detected in unchallenged flies (Fig. 1C-D), in keeping with the absence of visible peaks after MALDI-TOF analysis on collected hemolymph from unchallenged flies (Uttenweiler-Joseph et al., 1998). It is induced upon systemic infection by Gram-positive bacteria such as *Enterococcus faecalis* or by the fungus *Metarhizium robertsii* in two infection paradigms, injection of 50 conidia per fly or incubation of flies in a solution of spores at 5. 10^4/mL, the so-called "natural infection model" (Lemaitre et al., 1997). This induction is no longer observed in *MyD88* mutant flies in which Toll pathway signaling is abrogated (Fig. 1C), again consistent with MALDI-TOF data (Uttenweiler-Joseph et al., 1998). To determine whether the *BaraA* gene is involved in the host defense against infections, we gathered two independent Trip RNAi lines targeting this gene from the Tsinghua stock center (Ni et al., 2011). We also generated two independent CRISPR-Cas9 knock-out lines named KO-1 and KO-2 in which small deletions have been generated, which result in the predicted generation of truncated proteins (Fig. S1C-D). Finally, we also generated a knock-in (KI) mutant in which the *BaraA* coding sequence as well as the *CG30059* gene have been replaced by those encoding the mCherry fluorescent protein (Fig. S1A-B). When we monitored the expression of the *BaraA* gene in these different mutants after a *Micrococcus luteus* immune

challenge, we did not detect a significant induction of the gene for any of them (Fig. 1E). We also checked by MALDI-TOF analysis on collected hemolymph of immune-stimulated flies that we no longer observed the DIM peaks corresponding to the peptides derived from the processing of the BaraA protein. Fig. S2 shows that, unexpectedly, we nevertheless detect weak signals for DIM12, DIM10, and DIM13 for the two KD lines, and especially the KO2 line but not for the KI line. This phenomenon has been described previously for other KO lines made by CRISPR-Cas9 (El-Brolosy et al., 2019; Ma et al., 2019; Smits et al., 2019).

The BaraA *mutant is susceptible to* E. faecalis *infection*

We first tested the KD RNAi mutant lines in a survival assay after the injection of about 100 *E. faecalis* bacteria per fly. Under these conditions, about 60% of "wild-type" *w* A5001 flies survive whereas *MyD88* mutant flies succumb within a day. The KD flies displayed an intermediate phenotype, with about 40% of the flies surviving the challenge after 12 days (Fig. 2A). When we monitored the bacterial burden of the flies 24h after the inoculation, we noted a slightly increased bacterial load by a factor of 2. 1 to 2.5 (Fig. 2C). Unexpectedly, we obtained strikingly differing results for the KO and KI mutants: only the KO-1 mutant flies were susceptible to the infection whereas the other two lines survived at least as well as the *yw* control line (the background in which the KO and KI lines have been initially generated) (Fig. S3A-B). To resolve this unexpected difficulty, we isogenized all the KO and KI lines in the *w* A5001 background and repeated the experiments. As shown in Fig. 2B, the mutant lines now displayed a similar intermediate sensitivity phenotype, in keeping with the results obtained with the RNAi KD lines. However, we did not detect any significant difference in the bacterial burden at early or later time points of the infection between the isogenic A5001 control and the mutant lines (Fig. 2E-F). We also measured the bacterial load upon death and found no difference between

the lines, isogenized or not, suggesting that control and mutant flies succumb to the same level of bacterial proliferation (Figs. 2D, S3C).

As the KI mutant also removes the *CG18278* gene, we tested whether this gene might be involved in host defense against *E. faecalis*, even though it does not appear to be strongly induced by *E. faecalis* (Fig. S4A-B) and is expressed at a very low basal level (Flybase http://flybase.org/reports/FBgn0260475). We generated two independent KO lines by CRISPR-Cas9-mediated mutagenesis (Fig. S4C-D) that lead to the predicted formation of truncated proteins. As for a RNAi KD line, we did not observe any significantly enhanced sensitivity to injected *E. faecalis* bacteria (Fig. S4E-F).

The *BaraB* gene encodes another Baramicin gene family member with the DIM24 and DIM12/DIM10/truncated DIM13 domains; it lacks a predicted signal peptide (Fig. 1A). It is expressed at very low levels (http://wwww.flybase.org/reports/FBgn0033353) and is not induced by immune challenges (Fig. S5A-B). We also generated two KO mutants by CRISPR-Cas9-mediated mutagenesis that disrupt the reading frame (Fig. S5C-D). These mutant lines, as well as a RNAi KD line, did not display any difference with the control lines in *E. faecalis* survival experiments (Fig. S5E-F).

We conclude that only the *BaraA* mutant line displays an intermediate sensitivity to *E. faecalis* infection and does not show a strongly altered bacterial burden. Our experiments may however not be precise enough to exclude a mild difference in the bacterial loads, as illustrated in the KD experiments (Fig. 2C).

The BaraA *mutant is susceptible to* M. robertsii *infection only in the septic injury model*

When we tested the two KD RNAi lines, we did not detect any enhanced susceptibility to *M. robertsii* infection after injection (Fig. 3A), a finding also made with the nonisogenized KI line (Fig. S3D). In contrast, the nonisogenized KO-1 line exhibited a high sensitivity to the injected

conidia (Fig. S3E). We therefore tested the isogenized KO and KI lines. As shown in Fig. 3B, the three lines displayed an intermediate sensitivity to this fungal infection. As for *E. faecalis*, we did not detect any significant difference between wild-type and KO/KI lines as regards the fungal burden during the infection (Fig. 3C). Wild-type and mutant flies also succumbed to an average fungal load ranging from about 22,000 colony-forming units for *MyD88* flies to 100,000 cfus for KO-1, with however no significant differences in the distributions (Fig. 3D). There was thus no detectable difference in the fungal load upon death in this infection model.

We also exposed *BaraA* mutant flies to *M. robertsii* conidia in solution, the "natural" infection model, and did not observe any susceptibility phenotype with either the isogenized KO and KI mutants nor with the KD mutants (Fig. S6B-C). We conclude that the infection route is important as regards the susceptibility of *BaraA* to an entomopathogenic fungus.

Next, we challenged the *BaraA* mutant lines with the Gram-positive bacterium *Staphylococcus albus* and did not observe any enhanced sensitivity to this infection (Fig. S6A). Similar results were obtained when we injected several fungal pathogens (*Aspergillus fumigatus*; *Candida glabrata,* or *Candida albicans*, Fig. S6C-E) or Gram-negative bacteria (*Pectobacterium carotovorum,* formerly known as *Erwinia carotovora*, *Ecc15* strain and *Pseudomonas aeruginosa* PAO1 strain; Fig. S7A-C). As the infection route made a difference in the case of *M. robertsii* infection, we also tested PAO1 in an intestinal infection model in which bacteria escape the gut compartment and ultimately cause a generalized bacteremia (Haller et al., 2018; Limmer et al., 2011). *BaraA* isogenized KO and KI mutant lines also did not display any increased susceptibility when compared to the control line (Fig. S7D).

The conclusion from this limited analysis is that *BaraA* is required in the host defense against some but not all Gram-positive bacteria and entomopathogenic fungi.

An overexpression strategy fails to confer an enhanced protection against several pathogenic bacteria or fungi

A complementary strategy to the loss-of-function analysis reported above consists in overexpressing the *BaraA* gene in a wild-type context thus determining whether it might constitute a limiting factor in host defense against infections. To this end, we generated several transgenes allowing the overexpression using the Gal4/UAS system (Brand and Perrimon, 1993) of either the full-length BaraA protein, or some of its derived peptides, namely DIM24, DIM12, DIM10, and DIM13, with or without a HA tag. We checked by RTqPCR that the genes were indeed overexpressed when crossed to the strong ubiquitous driver *Ubi*-Gal4 and then also collected hemolymph from the overexpressing flies. As compared to *M. luteus*-challenged control flies, we detected higher peaks for detectable BaraA-derived DIM peptides.

E. faecalis, *M. robertsii*, and to a much more limited extent *Ecc15* bacteria, are able to kill wild-type flies. The different overexpression lines did not display any increased resistance to these challenges (Fig. S8C). We also checked that the overexpression of BaraA did not alter the resistance of wild-type flies to *A. fumigatus, C. albicans*, and *C. glabrata*.

The next question was whether the overexpression of BaraA or its derived peptides would rescue the high sensitivity phenotype to the infections listed above of the Toll pathway mutant *MyD88*. After a *M. luteus* or PBS challenge of *BaraA*-overexpressing flies in a *MyD88* mutant background, we observed by MALDI-TOF MS peaks for DIM24, DIM12, DIM10, and DIM13 but not for the smaller peptides DIM5, DIM6, and DIM8 (Fig. S8A-B). We conclude that the processing of the precursor BaraA into DIM peptides by a furin-like activity is not dependent on Toll pathway activation. In contrast, the processing of DIM12 and DIM13 into respectively DIM6 on the one hand and DIM5 and DIM8 on the other by a carboxypeptidase requires Toll signaling. Also, the stability of the BaraA-derived short DIMS does not require Bombardier since this protein is not induced in Toll pathway mutants (Lin et al., 2019).

We did not observe any rescue of the *MyD88* lethality induced by the six bacterial and fungal infections (Fig. S8C). Of note, the *BaraA* overexpression transgene rescued the *BaraA* KO mutant phenotype of sensitivity to *M. robertsii* and *E. faecalis* infections, thus demonstrating that the transgene is indeed functional (Fig. S8D-E), a result in keeping with the results obtained with the different *BaraA* mutants that indicated that the sensitivity phenotype to these two infections is due to the *BaraA* locus. We conclude that the genetic overexpression of *BaraA* is not sufficient to confer protection against *E. faecalis* or *M. robertsii*, in the context of a wild-type or Toll-deficient immune response.

We tested whether the synthetic peptides DIM12 and DIM13 display any antibacterial activity. We therefore incubated the peptides in micro-wells containing about 30,000 *E. faecalis* bacteria in Luria-Bertani broth. Whereas incubation with a scrambled DIM12 peptide or low, 1 to 2 mM, concentrations of the DIM12 peptide did not impair the growth of *E. faecalis*, higher concentrations from 3 mM onwards stopped the proliferation of *E. faecalis*. Of note, the 3mM concentration did not initially impair much the growth of the bacterium for the first 12 hours, the titer of the solution dropped afterwards. In contrast, the 100 µM gomesin positive control killed *E. faecalis* efficiently (Fig. S9). One experiment performed with DIM13 yielded a similar result.

These data establish that some of the DIM peptides display antibacterial activity at high concentrations, which are however unlikely to be found *in vivo* in the hemolymph.

BaraA does not modulate the induction of the Toll pathway

Besides a potential role of effectors, proteins that are induced by immune signaling pathways may play a role in feed-back regulation of the signaling pathway. We therefore monitored Toll pathway activation using the steady-state mRNA levels of AMP genes known to be regulated by the Toll pathway such as Drosomycin, Metchnikowin, and IM1 (Busse et al., 2007; Lemaitre

et al., 1996). As shown in Fig. 4A-C and Fig. S10, we did not observe any influence of the *BaraA* KO or KI null mutations in isogenized flies or KD flies over 48 hours.

BaraA *is required for efficient melanization*

Another important humoral immune response is melanization, which depends on the cleavage of prophenol oxidase proteins (proPO) into mature PO enzymes that catalyze several steps in the chemical reactions that lead to the formation and deposition of melanin (Dudzic et al., 2019; Dudzic et al., 2015). The PPO cleavage is initiated by proteolytic cascades that activate the Hayan protease, which cleaves PPOs (Cerenius et al., 2010; Nam et al., 2012). We challenged flies by injecting *M. luteus* and monitored PPO cleavage on Western blots using a PPO1 antibody (a kind gift from Prof. E. Ling). Fig. 4D show that PPO is not cleaved as efficiently in isogenic *BaraA* KO and KI mutants as in wild-type flies, a result obtained in three out of four experiments. These data suggest that *BaraA* is required for efficient melanization.

BaraA *plays a role in the host defense mediated by plasmatocytes*

In the *BaraA* KI line, the endogenous gene is replaced by the *mCherry* gene and is thus under the control of *BaraA* upstream regulatory sequences. Of note, because the KI line we obtained also removes the neighboring *CG30059* gene (Fig. S1A), *mCherry* expression would not be regulated by any sequence located downstream of the *BaraA* gene. We examined the expression of *mCherry* in nonchallenged and immune challenged flies by monitoring its fluorescence. In unchallenged adult flies, we noted a weak expression in some cells in the abdominal cuticle, with an enrichment of the signal in the dorsal vessel region suggesting these cells may therefore correspond to hemocytes (Fig. S11A). Of note, the reporter gene may also be expressed in pericardial cells. In contrast, upon challenge with *E. faecalis*, there was a strong induction of

mCherry fluorescence in the fat body (Fig. S11A). We also noted some expression in the head in challenged flies that may be linked to the cephalic fat body; we did not observe any expression in the brain of unchallenged larvae. We functionally tested whether the expression in the fat body was important for the role played by *BaraA* in host defense. To this end, we drove the expression of a *BaraA* KD line in the fat body using two Gal4 drivers expressed in the fat body (*yolk protein 1*-Gal4 [referred to here as yolk-Gal4] and *ppl*-Gal4). Whereas the yolk driver did not yield a *E. faecalis* sensitivity phenotype in survival experiments, we obtained a phenotype with the *ppl*-Gal4 driver (Fig. S11B-C). The basis for this divergent behavior is not easily accounted for as both Gal4 lines drive GFP expression quantitatively to similar levels (Huang *et al*., *in preparation*), except that *ppl* is expressed already at the larval stage, also in hemocytes (Tattikota et al., 2020), whereas *yolk protein 1* is expressed only in adult females.

The observation on adult abdomens suggested that hemocytes might be expressing *BaraA*. We therefore collected the hemolymph from nonchallenged and *E. faecalis*-injected flies and observed under the fluorescence microscope the expression of mCherry in hemocytes. A signal was detected in all the hemocytes of naive flies and was stronger upon immune challenge (Fig. 5A). We next asked whether knocking down *BaraA* expression specifically in hemocytes with the *hml* driver would impair the host defense against infections. Interestingly, we found that these flies were susceptible to an *E. faecalis* challenge (Fig. 5B) but not to injected *M. robertsii* conidia (Fig. 5E).

We then measured whether the uptake of Ph-RODO labelled *E. faecalis* bacteria is impaired in the isogenized *BaraA* KO null mutants. The number of fluorescent bacteria, which are presumably residing in mature acidified phagosomes, was not different in the KO flies as in the control (Fig. 5C-D). Of note, because in this assay the bacteria are killed, we cannot exclude

that live bacteria might interact differentially between wild-type or *BaraA* mutant plasmatocytes.

We also performed a phagocytic assay with injected live *M. robertsii* conidia, monitoring their uptake by plasmatocytes using a differential staining procedure in which the hemocytes are first incubated with an antiserum raised against *M. robertsii* spores and a secondary Alexa Fluor 555-labeled antibody (Wang *et al., in preparation*) in the absence of permeabilization and then performing the same staining, this time with an Alexa Fluor 488-labeled secondary antibody after permeabilization (Fig. 5E). Internalized conidia fluoresce green whereas spores outside of hemocytes appear yellow as they are stained in both steps of the procedure. Unexpectedly given the results obtained with the KD of *BaraA* in hemocytes, we found that the phagocytosis of *M. robertsii* is impaired in *BaraA KO* mutants. As BaraA secreted by the fat body or the hemocytes is matured in peptides, it is an open possibility that one or some of them actually act as opsonins to promote the uptake of *M. robertsii* conidia.

In conclusion, BaraA appears to be differentially required in the cellular host defense between *E. faecalis* and *M. robertsii*.

Baramicin A *does not appear to be involved in protecting the function of Malphigian tubules nor in the control of metabolic stores during infection*

As the *BaraA* mutants do not exhibit dramatically enhanced microbial burdens upon infections (Fig. 2C-D, Fig. 3C-D), we wondered whether *BaraA* might be involved in the resilience to infections. We first tested whether the excretory function of Malpighian tubules was affected earlier in *BaraA* mutants using the FRUMS assay (Franchet et al., 2019; Li et al., 2020). Fig. S12 shows that Malpighian tubule function deteriorated during *M. robertsii* infection at the same rate in wild-type and isogenized KO and KI *BaraA* mutants.

We next monitored the levels of triacylglycerides, glycogen, and glucose in wild-type and isogenized *BaraA* KO and KI mutants during *E. faecalis* and *M. robertsii* infection and did not find any significant difference between these lines in terms of metabolic stores, at least 24 hours after the beginning of the infection (Fig. S12 B-D).

DISCUSSION

We report here that the *BaraA* gene is required for host defense against two specific infections in a septic wound infection model, the Gram-positive pathogen *E. faecalis* and the entomopathogenic fungus *M. robertsii*. The *BaraA* mutants exhibit an intermediate sensitivity to these infections, with survival rates usually located halfway between wild-type and the highly sensitive Toll pathway mutant *MyD88*. In contrast to the latter mutant, we did not detect an enhanced growth and proliferation of the pathogens in the *BaraA* mutants, even though we found an impaired activation of melanization and phenotypes related to the cellular immune response. These complex and specific phenotypes have not been reported so far for genes regulated by the Toll pathway.

The sensitivity of BaraA *mutants to infection is restricted to a limited set of bacterial and fungal pathogens in a specific infection model*

We have tested a panel of pathogens known to kill more easily Toll pathway mutants. As regards Gram-positive bacteria, we have tested, besides *E. faecalis* and *S. albus, S. citreus*, α and ß-hemolytic Streptococci in a pilot experiment and failed to detect any sensitivity. With respect to fungal infections, we have also tested in the pilot screen *Talaromyces marneiffei* without success. We did not observe any sensitivity to the filamentous fungus *A. fumigatus* nor to the opportunistic pathogenic yeasts *C. albicans* and *C. glabrata*. At this stage, *BaraA* mutants

have been found to be susceptible only to two pathogens, *E. faecalis* and *M. robertsii*. As regards AMPs, it has been shown that some of them such as Diptericin and Drosocin appear to be required only for host defense against single bacterial pathogens, respectively *Providencia rettgeri* and *Enterobacter cloacae* (Hanson et al., 2019a; Unckless et al., 2016). BaraA thus constitutes a novel class of potential immune response effector that is required for host defense against specific species of Gram-positive bacteria on the one hand and fungi on the other, a protein with dual antimicrobial roles.

A noticeable finding from this study is that *BaraA* mutants exhibit a susceptibility to *M. robertsii* in the septic injury model and not in the "natural" infection model whereby conidia manage to pierce the cuticle. This behavior can be accounted by the difference of the pathology exerted by this pathogen according to its infection route, which involves different morphologies of the fungus and elicit marked differences in the relevant immune responses (Wang *et al*., in preparation). For instance, melanization is a moderately effective defense only in the septic injury model, which is apparently impaired in *BaraA* mutants.

One unsolved puzzle in our understanding of systemic humoral immunity is why there is a common signaling pathway, Toll, to regulate the response to drastically different pathogens such as Gram-positive bacteria and fungi, which are unlikely to be affected by the same effectors. Indeed, while AMPs such as Cecropins are active on Gram-negative bacteria and fungi *in vitro* (Ekengren and Hultmark, 1999; Hultmark et al., 1980; Tzou et al., 2002), there is no major influence of *bona fide* AMPs in the *D. melanogaster* host defense active against both fungi and Gram-positive bacteria (Hanson et al., 2019a; Rutschmann et al., 2000). BaraA thus provides a first but limited link for a common defense against the two categories of pathogens.

Is BaraA involved in resistance against infections?

The very structure of BaraA that encodes multiple repeats of a peptidic motif suggests that the concentration of DIM peptides achieved by the processing of the precursor is an important parameter. Indeed, the BaraA/ CG18278 locus is duplicated in some *D. melanogaster* lines and the gene is also found in two copies in the *melanogaster* subgroup while only one copy is found in some members of the other groups of the Drosophilinae subfamily, except for *D. virilis* in which a duplication of the locus occurred (Figs. S13-S14). Of note, in the case of *C. glabrata* infections, the BomS peptides also appear to be needed in high concentrations (Lindsay et al., 2018). In this case, the peptide copy number is increased by the selection for six independent genes, which are nevertheless clustered in the same locus at 55C (Clemmons et al., 2015).

DIM12 and DIM10 peptides are strongly cationic (Fig. 1A), a property found in AMPs that allow them to interact with the somewhat more negatively charged membranes of the microbes. We have found that high, millimolar, concentrations of the DIM12 peptide also prevent the growth of *E. faecalis*. Taken together, these properties are compatible with an antimicrobial activity of some DIM peptides, although the concentrations needed are unlikely to be found in the hemolymph (Drosomycin, a highly expressed AMP, was found to be present at a 0.3 mM concentration and identified in a differential screen(Fehlbaum et al., 1995): a peptide in even higher concentrations would likely not have been missed). Of note, any such antimicrobial activity is likely not targeted at common microbial processes, but at specific weaknesses of pathogens as has been previously described for Diptericin and Drosocin (Hanson et al., 2019a; Unckless et al., 2016).

BaraA is required for a full activation of the melanization defense since the maturation of proPO1 is not as efficient in *BaraA* as in wild-type control flies. Also, the uptake of *M. robsertsii* conidia by macrophages is less efficient. Thus, two known mechanisms of resistance to infection are impaired in *BaraA* loss-of-function mutants.

Both *E. faecalis* and *M. robertsii* pathogens grow and proliferate faster in Toll pathway mutants, an indication that this signaling pathway plays an important role in resistance against these infections. The finding of a potential antimicrobial action of BaraA-derived peptides as well as an involvement in the melanization and cellular host defenses that form part of the resistance arm of host defense would be predicted to lead to an increased microbial burden that was not observed consistently in our experiments. At best, we observed a two to four-fold increase in *E. faecalis* titer in *BaraA* KD flies (Fig. 2C), which was not detected in isogenized KO and KI flies. However, since the sensitivity phenotype to both *E. faecalis* and *M. robertsii* is rather mild, it is difficult to forecast which degree of microbial burden alteration one should expect and whether our techniques would be sensitive enough to detect milder modifications than two-fold reliably.

In conclusion, we cannot formally reject the hypothesis of a role for BaraA in the resistance against these infections; however, should it exist, this role would be rather limited or spatially restricted.

Is BaraA *involved in resilience to infections?*

This arm of host defense remains poorly investigated at present and in contrast to resistance may involve a variety of physiological mechanisms. We have documented here a few biological processes such as excretion by Malpighian tubules and also have checked that major metabolic stores during infections are not impacted by the *BaraA* KO or KI mutations. An indication of a role in resilience would be provided by altered microbial loads upon death (BLUD and FLUD), which we did not detect. Again, we cannot formally exclude that our analyses are not sensitive enough to reliably detect mild BLUD and FLUD phenotypes that would possibly mirror the moderate susceptibility to infections.

Altogether, our study does not point for a major role of BaraA in resilience to *E. faecalis* and *M. robertsii* infections but is compatible with a role in resistance that is not marked however.

The role of BaraA *in the cellular immune response*

A striking result is that *BaraA* is playing a role in the cellular response to both infections, but likely by distinct mechanisms. The KD of *BaraA* in hemocytes does not impact the survival to injected *M. robertsii* conidia in contrast to the situation for *E. faecalis* infections in which these hemocyte-*BaraA* KD flies are as susceptible as null mutant flies. The discovery that the plasmatocytes of *BaraA* mutants have a lessened ability to ingest *M. robertsii* conidia suggests that some BaraA-derived peptides produced by the fat body may function as opsonins. It is possible that BaraA participation in phagocytosis and melanization confers a mild protection against injected *M. robertsii* conidia that are coming in contact with hemocytes, which would however not be strong enough to warrant a detectable increase of the global fungal load when impaired.

Even though *BaraA* is required to be expressed in hemocytes, we did not detect any decreased uptake of PhRODO-labelled *E. faecalis* bacteria. Of note, this test may-be less reliable than the one we used for *M. robertsii* conidia because the microorganisms are killed. The strong phenotype of *hml-Gal4>BaraA* RNAi flies must be accounted for independently of phagocytosis. We propose that hemocytes may produce locally very high concentrations of BaraA-derived peptides that may kill or affect microorganisms at short range only. Interestingly, there might be a precedent in the *Drosophila* immune response: Cecropins cannot be detected in the cell-free hemolymph of flies, likely because the peak is suppressed from the neighboring one from Drosomycin, but can readily be detected in extracts from hemocytes (Uttenweiler-Joseph, 1998). The expression of *BaraA* may protect organs or tissues associated with hemocytes during infection that are critically targeted by *E. faecalis*. This hypothesis is in

keeping with a recently proposed antimicrobial role of neuropeptides that would provide locally protection to tissues (Brogden et al., 2005). We note that in unchallenged flies, hemocytes are mainly associated with the tracheal system and to a lower extent with the cardiac tube (Sanchez Bosch et al., 2019). As stated above, this type of strategy may however not significantly reduce the overall bacterial burden during infection yet may provide a degree of protection against infection that would be mirrored in the mild survival to *E. faecalis* infection phenotype. A corollary of this hypothesis is that other pathogens would target distinct tissues or organs or alternatively be resistant to the action of BaraA-derived peptides.

In conclusion, we propose that BaraA confers a degree of protection against *E. faecalis* and *M. robertsii* by acting locally close to hemocytes through distinct cell-autonomous and noncell-autonomous mechanisms.

Is BaraA acting alone in host defense?

A puzzling observation is that we observed differing phenotypes (survival, microbial burden, expression of AMP genes) in the various mutant lines we generated. These discrepancies disappeared upon isogenization, suggesting a strong contribution from the genetic background. Indeed, several genes have been identified by genome-wide association studies on *E. faecalis* and entomopathogenic fungi (Chapman et al., 2020; Wang et al., 2017).In addition, we did not observe any protection conferred by the transgenic overexpression of *BaraA*, in wild-type or *MyD88* background. It is thus likely that BaraA acts in conjunction with other Toll pathway-induced genes. Because the loss-of-function of *BaraA* is mild, a promising strategy will be to combine the null mutation with those affecting other Toll-dependent genes such as *Daisho, AMP* genes or single Bomanin genes at the 55C locus.

In summary, the present work provides novel insights into the function of Toll-regulated genes in host defense against one Gram-positive bacterium and one entomopathogenic fungus and

underscores the complexity of the different levels of host defense, some of which may act only locally even in the context of a systemic infection. While the present study failed to ascribe a specific function to any of the BaraA-derived peptides that have been studied using our genetic overexpression strategy that remained limited to the analysis of the survival to infection phenotype, future work focusing on specific host defenses affected in *BaraA* mutants coupled to a combinatorial strategy may yield novel insights in the function of this precursor protein.

Materials and Methods

MATERIALS AND METHODS

Fly strains

D. melanogaster fly strains were maintained at 25°C with 12hour light/dark cycles and fed standard cornmeal-molasses-agar fly medium. The recipe for 1L is as follows: Agar 9g, yeast 32.19g, $CaCl_2$ 0.726g, sucrose 31.62g, glucose 63.2g, corn flour 77.7g, potassium sorbate 2g, 15 mL of a 100g ethyl p-hydroxybenzoate dissolved in 1L absolute ethyl alcohol solution, qsp 1L distilled water.

w A5001 and *yw* flies were used as wild type controls. The positive controls for infection assays for Gram-positive/fungal infections and Gram-negative infections were respectively *MyD88* and *key*. For isogenic flies, the wild type control came from the backcross which background was w^{A5001}. For RNAi experiments, virgin females carrying one of the following transposons: *Ubi-Gal4, tubP-Gal80^{ts}/ hmlΔ–Gal4, tubP-Gal80^{ts}, UAS-GFP/ yolk-Gal4/ ppl-Gal4* were crossed to males carrying UAS-RNAi transgenes (TRiP) from the Tsinghua RNAi Center or from the Bloomington stock center: THU0407 (*BaraA*-KD1), THU0393 (*BaraA*-KD2), BL-61998 (*BaraB* KD), and THU02336.N (*CG18278* KD). For TRiP RNAi flies, the control flies were *UAS*-mCherry RNAi VALIUM20 (number 35785). Crosses were performed at 25°C with the driver *Ubi-Gal4, Gal80^{ts}* for three days, then the progeny was left to develop at the non-

permissive 18°C temperature. The hatched flies were kept at 29°C for five days prior to the experiment to allow Gal4-mediated transcription. All crosses involving flies without RNAi expression were performed at 25 °C.

CRISPR/Cas9 Deletion

The *BaraA* (*CG18279*), *BaraB* (*CG13749*) and *CG18278* were using CRISPR/Cas9 technology according to the following protocols to generate the frame shift mutants. The 20bp-long gRNAs for the target genes were devised using web-based CRISPR Optimal Target Finder (http://targetfinder.flycrispr.neuro.brown.edu/), which was designed to enhance the specificity of the target sequence by comparing it to the whole Drosophila genome. To effectively disrupt gene function, the target was selected in a region as close as possible to the initiating ATG of the coding region. The plasmids carrying DNA sequences for the production of single strand gRNAs were constructed using standard methods. Briefly, the oligonucleotides were synthesized, denatured, and annealed to get double strand DNA before ligation into the expression vector, in which the gRNA coding sequences were transcribed under the control of the U6:3 promoter.

Plasmids carrying different gRNA targets were grouped by three or six for microinjection to obtain the gRNA transgenic fly lines, which were checked by sequencing. For the targeting genes located on the 1st and 2nd chromosomes, the gRNAs expressing plasmids were designed to be inserted on the 3rd chromosome using y^1 M{vas-int.Dm}ZH-2A w*; M{3xP3-RFP.attP}ZH-86Fb (BL24749) flies, whereas for genes of the 3rd chromosome, the transgenes were inserted on the 2nd chromosome using y^1M{vas-int. Dm}ZH-2A w*; M{3xP3-RFP.attP'}ZH-51C (BL24482) flies. The gRNA flies were balanced before being crossed to flies carrying the *nosP-Cas9* transgene, to induce inheritable mutations. The primers we used to generate the knock out mutants show in Supplementary Table 1.

Knock-in strategy

PCRs were done with the Q5 Hot-start 2× master mix (New England BioLabs, NEB), and cloning was performed using the Gibson Assembly 2× Master Mix (NEB) following the manufacturer's instructions. The pCFD5 (U6:3-(t :: RNA^{Cas9})) plasmid vector was used. A cloning protocol to generate the pCFD5 plasmids encoding one to six tRNA-flanked sgRNAs was followed as described (Port and Bullock, 2016). The primers used to generate the pCFD5 vector containing the gRNAs are shown in Supplementary Table 1. We used a pSK vector as donor plasmid with the homology arms flanking the mCherry: a fragment 1552bp upstream of *BaraA* had been amplified as a left arm; a fragment1952bp downstream of *CG30059* as a right arm. Left arm + mCherry + right arm have been assembled (Gilson Assembly) and the resulting fragment ligated to Pst1-Spe1 double-digested pSK and checked by sequencing. The plasmid mixture containing the two plasmids at a ration pCFD5:pSK=3:1, was injected into recipient y^1 M{Act5C-Cas9.P.RFP-}ZH-2A w^{1118} DNAlig4^{169} embryos.

Overexpression strategy

Normal PCRs in first and second round were performed to amplify the ORF of BaraA OR BaraA derived peptides (DIM24, 12, 10, 13), constructing in pDONR221 with attP site (Bischof et al., 2014). The primers used are shown in Supplementary Table 1. BP recombination reaction was performed using with DH5α competent cells (Invitrogen); next, sequence-confirmed ORF entry clones were transferred to the destination vector pGW-HA.attB using a Gateway LR reaction (Gibson assembly). After validation by sequencing, the plasmids were injected in a pool into y^1 M{vas-int.Dm}ZH-2A w*; M{3xP3-RFP.attP}ZH-86Fb embryos and missing constructs were reinjected alone.

Pathogen infections

The bacterial strains used and their respective optical density of the pellet (OD) at 600 nm. The bacterial strains used in this study include Gram-negative *Pectinobacterium carotovorum carotovorum 15(strain ECC15,* OD=50*) Pseudomonas aeruginosa (PAO1,* OD=0.001*),* as well as the Gram-positive *Enterococcus faecalis* (OD=0.1), *Micrococcus luteus* (OD=200) and *Staphylococcus albus* (OD=10). The fungal strains we used include filamentous fungi, *Aspergillus fumigatus* (5*10^7/mL, 250spores in 4.6nl)*, Metarhizium robertsii* (10^7/mL, natural infection 5*10^4/mL)*, Talaromyces marneffei* (5*10^7/mL). Besides, we used yeast as well, *Candida albicans* (pricked) and *Candida glabrata* (10^9/mL). *PAO1* were cultured in Brain-Heart Infusion Broth (BHI-L), The following media were used to grow the strains: Yeast extract- Peptone-Glucose Broth Agar (YPDA, *C. albicans* and C. glabrata) or Luria Broth (LB - all others) at 29°C (*ECC15*, *M. luteus*, *C. albicans*, *C. glabrata*) or 37°C. Spores of entomopathogenic strains *M. robertsii*, *A. fumigatus* and *T. marneffei* were grown on Potato Dextrose Agar(PDA) plates at 25°C or 29°C (*A. fumigatus*) for approximately one weeks or three weeks (*A. fumigatus*) until sporulation. We injected 4.6 nL of the suspension into each fly thorax using a Nanoject Ⅲ (Drummond). Natural infections were initiated by shaking anesthetized flies in 5ml with 0.01% tween-20 containing *M. robertsii* conidia at a concentration of 5*10^4/mL. Infected flies were subsequently maintained at 29°C (*PAO1* injection, *C. albicans*, *C. glabrata*, *A. fumigatus, M. robertsii, T. marneffei*) or at 25°C (for all other pathogens, except for experiments with RNAi KD flies performed at 29°C). Flies were anesthetized with light CO2 for about three minutes during the injection procedure and were observed 3h after injection to confirm recovery from manipulations. Differences in survival were tested with Log-rank test.

Pathogen Load Quantification

To characterize the dynamics of within-host microbial loads or BLUDs or FLUDs, flies were infected with *E. faecalis* or *M. robertsii* and vials were monitored every 30 minutes for newly dead flies or live flies were taken at each time point post-injection for set point pathogen load. These flies were then individually homogenized with a bead in 100 µl PBS with 0.01% tween20 (PBST) or PBS. Homogenates were diluted serially in PBST (or PBS)and spread on LB(*E. faecalis*) or PDA(*M. robertsii*) plates for incubation at 37°C (*E. faecalis*) or 25°C (*M. robertsii*) overnight. Colonies were counted manually. Data were obtained from at least three independent experiments and pooled.

In vivo phagocytosis assay of E. faecalis pHrodo and live spores

The pHrodo dye becomes fluorescent when placed in an acidic environment such as that encountered in phagosomes. 4.6nl of the pHrodo dye was injected into female flies; after 40 min of incubation at 25°C, the abdomen of the flies was observed using a Zeiss fluorescent microscope. 10 flies of each line were scored in each experiment and three independent experiments were performed. WT or *ΔBaraA* mutants third-instar wandering larvae were injected with 27.6 nl of the live fungal solutions (3*10^8/ml) using a Nanoject apparatusⅢ (Drummond). After 2h of incubation at 29°C, live larvae were bled, each in a well of an 8-well microscopy slide that contained PBS. The cells were left to settle to the bottom of the well for 30 min and then were fixed in 2% paraformaldehyde for 10 min, in a humid chamber at room temperature. The fixed cells were washed twice in PBS, after 20min incubation in a PBS solution with 2% BSA(PBSB), the samples were stained with a 1/500 diluted rabbit antiserum against *M. robertsii* in a PBSB solution overnight at 4°C. The cells were incubated with an Alexa Fluor 555-labeled goat anti-rabbit secondary antibody (Invitrogen) in a PBSB for 2 h at room temperature. After 20min permeabilization step in a PBS solution with 0.1% Triton X-100 and 2% BSA (PBSBT), a second round of staining with the diluted rabbit antiserum against

M. robertsii in PBSBT was performed overnight at 4°C and afterwards washed twice with PBSBT. The samples were then incubated with an Alexa Fluor 488-labeled goat anti-rabbit secondary antibody (Invitrogen) in PBSBT for 2 h at room temperature and afterwards washed twice with PBSBT. The slides were mounted in Vectashield with DAPI (Vector Laboratories) and analyzed using a Zeiss fluorescent microscope. 50 cells per larva were analyzed: The number of green fluorescent fungus that were not also red (phagocytosed bacteria) was determined for each DAPI-positive hemocyte, and the phagocytosis index was calculated (percentage of phagocytes containing at least 1 only-green bacterium) × (mean number of only-green bacteria per phagocyte).

Gene Expression Quantitation

Total RNA was extracted from 5 adult flies collected at different time points after Toll activation with TRIzol (Invitrogen). cDNA was synthesized from 1000 ng total RNA using the SuperScript II Reverse Transcriptase kit (Transgene). Quantitative RT- PCR was performed on an iQ5 cycler (BioRad) using SYBR Green Supermix (Vazyme). Quantification of mRNA levels was calculated relative to levels of the ribosomal protein gene *rpl32*. See Supplemental Table 2_for qPCR primer sequences. Primer couples displayed a similar efficiency, which allowed us to use the ΔΔCt method to analyze the data.

Survival tests

Survival tests were performed using 20-25 flies per vial in biological triplicates. Adult flies used for survival tests were 5–7-days old. For survival tests using RNAi-silencing genes, flies crossed at 25°C for 3days for laying eggs then transferred to 18°C; after hatching, flies were kept for at least 5 days at 29°C prior to infections. Flies were counted every day. Each experiment shown is representative of at least two independent experiments.

Molecular mass fingerprints by MALDI MS

Sample preparation, data acquisition and processing

Each individual hemolymph sample was analyzed with the Bruker AutoFlex™ III based on Bruker Daltonics' smartbeam laser technology. The molecular mass fingerprints (MFP) were acquired using a sandwich sample preparation on a MALDI MTP 384 polished ground steel plate (Bruker Daltonics Inc., Germany). Briefly, the hemolymph samples were 10-fold diluted in acidified water (0.1% trifluoroacetic acid - 0.1% TFA, Sigma Aldrich, France), 0.6µL was deposited on a thin layer of an air dried saturated solution (0.6µL) of the matrix alpha-cyano-4-hydroxycinnamic Acid (4-HCCA, Sigma Aldrich, France) in pure acetone. Then 0.4 µL of a saturated solution of 4-HCCA prepared in 50% acetonitrile acidified with 0.1% TFA was mixed with the *Drosophila* haemolymph. Following co-crystallization of the hemolymph spots with the second matrix droplet and evaporation under mild vacuum, MALDI MS spectra were recorded in a linear positive mode and in an automatic data acquisition using FlexControl 4.0 software (Bruker Daltonics Inc.). The following instrument settings were used: the pseudo-molecular ions desorbed from the hemolymph were accelerated under 1.3kV, dynamic range of detection of 600 to 18,000 Da, between 50-60% of laser power, a global attenuator offset of 60% with 200Hz laser frequency, and 2,000 accumulated laser shots per hemolymph spectrum. The linear detector gain was setup at 1,906V with a suppression mass gate up to *m/z* 600 to prevent detector saturation by clusters of the 4-HCCA matrix. An external calibration of the mass spectrometer was performed using a standard mixture of peptides and proteins (Peptide Standard Calibration II and Protein Standard Calibration I, Bruker Daltonik) covering the dynamic range of analysis. All of the recorded spectra were processed with a baseline subtraction and spectral smoothing using FlexAnalysis 4.0 software (Bruker Daltonics Inc.).

Metabolite measurements

Female flies were first infected by 4.6nl *E. faecalis* or *M, robertsii* for 24 hours. Five flies per condition were used to measure the metabolite levels. Glycogen, glucose and triglycerides (TAGs) were measured using the Glycogen Assay Kit (700480), the Glucose Colorimetric Assay Kit (10009582), the Triglyceride Colorimetric Assay Kit (10010303 from Cayman Chemical), respectively. Standard curves were obtained according to the manufacturer's instructions. The flies selected for each experiment had approximately the same body weight.

Statistical analysis

Data are expressed as means ± SD. Data were analyzed by ANOVA (one-way) with Dunnett's multiple comparisons test, with a significance threshold of P = 0.05. Log-rank tests were used to determine whether survival curves of female flies were significantly different from each other. Details are included in the legend of each figure. *P < 0.05; **P < 0.01; ***P < 0.001; **** P<0.0001.

Acknowledgments

We thank our colleagues at the Sino-French Hoffmann Institute for help and advice at various steps of this work. We are grateful to Dr. Wenhui Wang and Prof. Erjun Ling for providing antibodies and the Bloomington and Tsinghua stock Centers for fly stocks. We would like to thank Sébastien Voisin from the BioPark for his help in mass spectrometry and Yongfang Zheng for expert technical help. We are indebted to the Guangzhou Drosophila Resource Center for the generation of CRISPR-Cas9 KO lines. This work was supported from the Association Platform BioPark of Archamps on its Research & Development budget, from grants from the Guangzhou Medical University and from the 1,000 Talent program to DF.

References

Bischof, J., Sheils, E.M., Bjorklund, M., and Basler, K. (2014). Generation of a transgenic ORFeome library in Drosophila. Nat Protoc *9*, 1607-1620.

Boutros, M., Agaisse, H., and Perrimon, N. (2002). Sequential activation of signaling pathways during innate immune responses in Drosophila. Dev Cell *3*, 711-722.

Brand, A.H., and Perrimon, N. (1993). Targeted gene expression as a means of altering cell fates and generating dominant phenotypes. Development *118*, 401-415.

Brogden, K.A., Guthmiller, J.M., Salzet, M., and Zasloff, M. (2005). The nervous system and innate immunity: the neuropeptide connection. Nat Immunol *6*, 558-564.

Buchon, N., Silverman, N., and Cherry, S. (2014). Immunity in Drosophila melanogaster--from microbial recognition to whole-organism physiology. Nat Rev Immunol *14*, 796-810.

Busse, M.S., Arnold, C.P., Towb, P., Katrivesis, J., and Wasserman, S.A. (2007). A kappaB sequence code for pathway-specific innate immune responses. Embo J *26*, 3826-3835.

Capilla, A., Karachentsev, D., Patterson, R.A., Hermann, A., Juarez, M.T., and McGinnis, W. (2017). Toll pathway is required for wound-induced expression of barrier repair genes in the Drosophila epidermis. Proc Natl Acad Sci U S A *114*, E2682-E2688.

Cerenius, L., Kawabata, S., Lee, B.L., Nonaka, M., and Soderhall, K. (2010). Proteolytic cascades and their involvement in invertebrate immunity. Trends Biochem Sci *35*, 575-583.

Chapman, J.R., Dowell, M.A., Chan, R., and Unckless, R.L. (2020). The Genetic Basis of Natural Variation in Drosophila melanogaster Immune Defense against Enterococcus faecalis. Genes (Basel) *11*.

Chapman, J.R., Hill, T., and Unckless, R.L. (2019). Balancing Selection Drives the Maintenance of Genetic Variation in Drosophila Antimicrobial Peptides. Genome biology and evolution *11*, 2691-2701.

Clemmons, A.W., Lindsay, S.A., and Wasserman, S.A. (2015). An effector Peptide family required for Drosophila toll-mediated immunity. PLoS Pathog *11*, e1004876.

Cohen, L.B., Lindsay, S.A., Xu, Y., Lin, S.J.H., and Wasserman, S.A. (2020). The Daisho Peptides Mediate Drosophila Defense Against a Subset of Filamentous Fungi. Front Immunol *11*, 9.

De Gregorio, E., Han, S.J., Lee, W.J., Baek, M.J., Osaki, T., Kawabata, S., Lee, B.L., Iwanaga, S., Lemaitre, B., and Brey, P.T. (2002). An immune-responsive Serpin regulates the melanization cascade in Drosophila. Dev Cell *3*, 581-592.

De Gregorio, E., Spellman, P.T., Rubin, G.M., and Lemaitre, B. (2001). Genome-wide analysis of the Drosophila immune response by using oligonucleotide microarrays. Proc Natl Acad Sci U S A *98*, 12590-12595.

Dudzic, J.P., Hanson, M.A., Iatsenko, I., Kondo, S., and Lemaitre, B. (2019). More Than Black or White: Melanization and Toll Share Regulatory Serine Proteases in Drosophila. Cell reports *27*, 1050-1061 e1053.

Dudzic, J.P., Kondo, S., Ueda, R., Bergman, C.M., and Lemaitre, B. (2015). Drosophila innate immunity: regional and functional specialization of prophenoloxidases. BMC Biol *13*, 81.

Duneau, D., Ferdy, J.B., Revah, J., Kondolf, H., Ortiz, G.A., Lazzaro, B.P., and Buchon, N. (2017). Stochastic variation in the initial phase of bacterial infection predicts the probability of survival in D. melanogaster. eLife *6*.

Duxbury, E.M., Day, J.P., Maria Vespasiani, D., Thuringer, Y., Tolosana, I., Smith, S.C., Tagliaferri, L., Kamacioglu, A., Lindsley, I., Love, L*., et al.* (2019). Host-pathogen coevolution increases genetic variation in susceptibility to infection. eLife *8*.

Ekengren, S., and Hultmark, D. (1999). Drosophila cecropin as an antifungal agent. Insect Biochem Mol Biol *29*, 965-972.

El-Brolosy, M.A., Kontarakis, Z., Rossi, A., Kuenne, C., Gunther, S., Fukuda, N., Kikhi, K., Boezio, G.L.M., Takacs, C.M., Lai, S.L*., et al.* (2019). Genetic compensation triggered by mutant mRNA degradation. Nature *568*, 193-197.

Fehlbaum, P., Bulet, P., Michaut, L., Lagueux, M., Brockaert, W.F., Hétru, C., and Hoffmann, J.A. (1995). Septic injury of *Drosophila* induces the synthesis of a potent antifungal peptide with sequence homology to plant antifungal peptides. J Biol Chem *269*, 33159-33163.

Ferrandon, D. (2013). The complementary facets of epithelial host defenses in the genetic model organism Drosophila melanogaster: from resistance to resilience. Curr Opin Immunol *25*, 59-70.

Ferrandon, D., Imler, J.L., Hetru, C., and Hoffmann, J.A. (2007). The Drosophila systemic immune response: sensing and signalling during bacterial and fungal infections. Nat Rev Immunol *7*, 862-874.

Franchet, A., Niehus, S., Caravello, G., and Ferrandon, D. (2019). Phosphatidic acid as a limiting host metabolite for the proliferation of the microsporidium Tubulinosema ratisbonensis in Drosophila flies. Nat Microbiol *4*, 645-655.

Haller, S., Franchet, A., Hakkim, A., Chen, J., Drenkard, E., Yu, S., Schirmeier, S., Li, Z., Martins, N., Ausubel, F.M.*, et al.* (2018). Quorum-sensing regulator RhlR but not its autoinducer RhlI enables Pseudomonas to evade opsonization. EMBO Rep *19*, e44880.

Hanson, M.A., Dostalova, A., Ceroni, C., Poidevin, M., Kondo, S., and Lemaitre, B. (2019a). Synergy and remarkable specificity of antimicrobial peptides in vivo using a systematic knockout approach. eLife *8*.

Hanson, M.A., Lemaitre, B., and Unckless, R.L. (2019b). Dynamic Evolution of Antimicrobial Peptides Underscores Trade-Offs Between Immunity and Ecological Fitness. Front Immunol *10*, 2620.

Hultmark, D., Steiner, H., Rasmuson, T., and Boman, H.G. (1980). Insect immunity. Purification and properties of three inducible bactericidal proteins from hemolymph of immunized pupae of Hyalophora cecropia. Eur J Biochem *106*, 7-16.

Irving, P., Troxler, L., Heuer, T.S., Belvin, M., Kopczynski, C., Reichhart, J., Hoffmann, J.A., and Hetru, C. (2001). A genome-wide analysis of immune responses in *Drosophila*. Proc Natl Acad Sci (USA) *98*, 15119-15124.

Lau, G.W., Goumnerov, B.C., Walendziewicz, C.L., Hewitson, J., Xiao, W., Mahajan-Miklos, S., Tompkins, R.G., Perkins, L.A., and Rahme, L.G. (2003). The Drosophila melanogaster toll pathway participates in resistance to infection by the gram-negative human pathogen Pseudomonas aeruginosa. Infect Immun *71*, 4059-4066.

Lazzaro, B.P. (2008). Natural selection on the Drosophila antimicrobial immune system. Curr Opin Microbiol *11*, 284-289.

Lemaitre, B., and Hoffmann, J. (2007). The Host Defense of Drosophila melanogaster. Annu Rev Immunol *25*, 697-743.

Lemaitre, B., Nicolas, E., Michaut, L., Reichhart, J.M., and Hoffmann, J.A. (1996). The dorsoventral regulatory gene cassette *spätzle/Toll/cactus* controls the potent antifungal response in *Drosophila* adults. Cell *86*, 973-983.

Lemaitre, B., Reichhart, J.M., and Hoffmann, J.A. (1997). Drosophila host defense : differential display of antimicrobial peptide genes after infection by various classes of microorganisms. Proc Natl Acad Sci USA *94*, 14614-14619.

Levy, F., Bulet, P., and Ehret-Sabatier, L. (2004a). Proteomic analysis of the systemic immune response of Drosophila. Mol Cell Proteomics *3*, 156-166.

Levy, F., Rabel, D., Charlet, M., Bulet, P., Hoffmann, J.A., and Ehret-Sabatier, L. (2004b). Peptidomic and proteomic analyses of the systemic immune response of Drosophila. Biochimie *86*, 607-616.

Li, X., Rommelaere, S., Kondo, S., and Lemaitre, B. (2020). Renal Purge of Hemolymphatic Lipids Prevents the Accumulation of ROS-Induced Inflammatory Oxidized Lipids and Protects Drosophila from Tissue Damage. Immunity *52*, 374-387 e376.

Ligoxygakis, P., Pelte, N., Ji, C., Leclerc, V., Duvic, B., Belvin, M., Jiang, H., Hoffmann, J.A., and Reichhart, J.M. (2002). A serpin mutant links Toll activation to melanization in the host defence of Drosophila. Embo J *21*, 6330-6337.

Limmer, S., Haller, S., Drenkard, E., Lee, J., Yu, S., Kocks, C., Ausubel, F.M., and Ferrandon, D. (2011). Pseudomonas aeruginosa RhlR is required to neutralize the cellular immune response in a Drosophila melanogaster oral infection model. Proc Natl Acad Sci U S A *108*, 17378-17383.

Lin, S.J.H., Fulzele, A., Cohen, L.B., Bennett, E.J., and Wasserman, S.A. (2019). Bombardier Enables Delivery of Short-Form Bomanins in the Drosophila Toll Response. Front Immunol *10*, 3040.

Lindsay, S.A., Lin, S.J.H., and Wasserman, S.A. (2018). Short-Form Bomanins Mediate Humoral Immunity in Drosophila. J Innate Immun *10*, 306-314.

Longdon, B., Hadfield, J.D., Day, J.P., Smith, S.C., McGonigle, J.E., Cogni, R., Cao, C., and Jiggins, F.M. (2015). The causes and consequences of changes in virulence following pathogen host shifts. PLoS Pathog *11*, e1004728.

Ma, Z., Zhu, P., Shi, H., Guo, L., Zhang, Q., Chen, Y., Chen, S., Zhang, Z., Peng, J., and Chen, J. (2019). PTC-bearing mRNA elicits a genetic compensation response via Upf3a and COMPASS components. Nature *568*, 259-263.

McKean, K.A., Yourth, C.P., Lazzaro, B.P., and Clark, A.G. (2008). The evolutionary costs of immunological maintenance and deployment. BMC Evol Biol *8*, 76.

Medzhitov, R., Schneider, D.S., and Soares, M.P. (2012). Disease tolerance as a defense strategy. Science *335*, 936-941.

Nam, H.J., Jang, I.H., You, H., Lee, K.A., and Lee, W.J. (2012). Genetic evidence of a redox-dependent systemic wound response via Hayan protease-phenoloxidase system in Drosophila. Embo J *31*, 1253-1265.

Ni, J.Q., Zhou, R., Czech, B., Liu, L.P., Holderbaum, L., Yang-Zhou, D., Shim, H.S., Tao, R., Handler, D., Karpowicz, P.*, et al.* (2011). A genome-scale shRNA resource for transgenic RNAi in Drosophila. Nat Methods *8*, 405-407.

Port, F., and Bullock, S.L. (2016). Augmenting CRISPR applications in Drosophila with tRNA-flanked sgRNAs. Nat Methods *13*, 852-854.

Rutschmann, S., Jung, A.C., Rui, Z., Silverman, N., Hoffmann, J.A., and Ferrandon, D. (2000). Role of *Drosophila* IKKg in a Toll-independent antibacterial immune response. Nat Immunology *1*, 342-347.

Sackton, T.B., Lazzaro, B.P., Schlenke, T.A., Evans, J.D., Hultmark, D., and Clark, A.G. (2007). Dynamic evolution of the innate immune system in Drosophila. Nat Genet *39*, 1461-1468.

Sanchez Bosch, P., Makhijani, K., Herboso, L., Gold, K.S., Baginsky, R., Woodcock, K.J., Alexander, B., Kukar, K., Corcoran, S., Jacobs, T.*, et al.* (2019). Adult Drosophila Lack Hematopoiesis but Rely on a Blood Cell Reservoir at the Respiratory Epithelia to Relay Infection Signals to Surrounding Tissues. Dev Cell *51*, 787-803 e785.

Smits, A.H., Ziebell, F., Joberty, G., Zinn, N., Mueller, W.F., Clauder-Munster, S., Eberhard, D., Falth Savitski, M., Grandi, P., Jakob, P.*, et al.* (2019). Biological plasticity rescues target activity in CRISPR knock outs. Nat Methods *16*, 1087-1093.

Soares, M.P., Teixeira, L., and Moita, L.F. (2017). Disease tolerance and immunity in host protection against infection. Nat Rev Immunol *17*, 83-96.

Tattikota, S.G., Cho, B., Liu, Y., Hu, Y., Barrera, V., Steinbaugh, M.J., Yoon, S.H., Comjean, A., Li, F., Dervis, F.*, et al.* (2020). A single-cell survey of Drosophila blood. eLife *9*.

Troha, K., Im, J.H., Revah, J., Lazzaro, B.P., and Buchon, N. (2018). Comparative transcriptomics reveals CrebA as a novel regulator of infection tolerance in D. melanogaster. PLoS Pathog *14*, e1006847.

Tzou, P., Reichhart, J.M., and Lemaitre, B. (2002). Constitutive expression of a single antimicrobial peptide can restore wild-type resistance to infection in immunodeficient Drosophila mutants. Proc Natl Acad Sci U S A *99*, 2152-2157.

Unckless, R.L., Howick, V.M., and Lazzaro, B.P. (2016). Convergent Balancing Selection on an Antimicrobial Peptide in Drosophila. Curr Biol *26*, 257-262.

Uttenweiler-Joseph, S. (1998). La spectrométrie de mase MALDI-TOF comme nouvelle approche méthodologique pour l'étude de la réponse immunitaire des insectes (Université Louis Pasteur de Strasbourg).

Uttenweiler-Joseph, S., Moniatte, M., Lagueux, M., Van Dorsselaer, A., Hoffmann, J.A., and Bulet, P. (1998). Differential display of peptides induced during the immune response of Drosophila: a matrix-assisted laser desorption ionization time-of- flight mass spectrometry study. Proc Natl Acad Sci U S A *95*, 11342-11347.

Wang, J.B., Lu, H.L., and St Leger, R.J. (2017). The genetic basis for variation in resistance to infection in the Drosophila melanogaster genetic reference panel. PLoS Pathog *13*, e1006260.

Figure legends

Fig. 1: Structure of the BaraA precursor protein and induction of its expression by an immune challenge.

(A) Schematic structure of the Bara family members BaraA and BaraB. The name of the genes encoding the proteins is indicated below the protein names, *BaraA* being duplicated. The sites of internal processing at furin-like cleavage sites are indicated by orange and yellow arrows. The name of the peptides derived from the processing of the precursor are shown. Please, note that BaraB lacks a signal peptide and may therefore not be secreted. (B) Alignment of the short DIM peptides, referred to by their numbers, derived from BaraA and BaraB, aligned to each

other within a protein on the left side and aligned to the corresponding domain in the other Bara protein on the right side. (C) Expression of the *BaraA* gene monitored by RTqPCR at various time points after the injection of the indicated microbes; *M. lu*: *M. luteus; M. r: M. robertsii*; *E. fa: E. faecalis*. (D) Expression of the *BaraA* gene monitored by RTqPCR at 24 and 48 hours after a "natural" infection achieved by plunging the flies in a solution of *M. robertsii* conidia (E) *BaraA* expression level measured by RTqPCR in wild-type (WT), *BaraA* knock down (KD), knock out (KO), knock in(KI), and *MyD88* flies, challenged by *M. luteus* for 24hours.

Fig. 2: BaraA mutant flies are susceptible to *E. faecalis* infection.

(A) Survival of *ubi-Gal4, Gal80^{ts}>BaraA* RNAi KD1 and KD2 flies injected each with about 100 *E. faecalis* bacteria; one representative experiment out of 13. Statistical significance was determined using the Log-rank test, *P < 0.05, **P < 0.01 (B) Survival curves of the isogenic *BaraA* KO and KI flies infected with *E. faecalis*; one representative experiment out of 5. The WT corresponds to a wild type *w* A5001 line isogenized in parallel to the KO and KI lines, which behaves like the *w* A5001 line used for isogenization. *P < 0.05 (C) Bacterial titer of the hemolymph collected from *BaraA* KD flies 24 hours post-infection. Pooled data from three independent experiments, ANOVA with Dunett's post-hoc tests *P < 0.05 ***P < 0.001 (D) Bacterial load upon death (BLUD) of (E, F) by *E. faecalis*, from early time points (E) to days 1 to 6 after infection (F). No significant difference was detected between WT and mutants at each time point. Pooled data from three independent experiments.

Fig. 3 *BaraA* mutant flies are susceptible to *M. robertsii* infection.

(A) Survival of *ubi-Gal4, Gal80^{ts}>BaraA* RNAi KD1 and KD2 flies injected each with about 250 *M. robertsii* conidia per fly. No significant difference between wild type and KD flies was detected in six out of nine experiments. (B) Isogenic *BaraA* mutants injected with 250 *M.*

robertsii conidia. KO1, KO2 and KI performance were consistent; one representative experiment out of 7. Statistical significance between WT and the KO or KI mutants: ***P < 0.001. (C) Kinetics over three days of the fungal load of the *BaraA* KO and KI mutants injected with 250 *M. robertsii* conidia. No significant difference was detected between WT and mutants at each time point. (D) Fungal load upon death (FLUD) of single isogenic *BaraA* KO and KI flies injected with 250 *M. robertsii* conidia. The fungal burden was measured within 30 minutes following the demise of the single flies. No significant difference between WT and the isogenic mutant flies was detected. Three independent experiments have been performed and pooled (C-D).

Fig. 4 ***BaraA* does not affect with the induction of the expression of Toll-regulated genes by an immune challenge but interferes with the maturation of proPO1 into an active melanization enzyme.**

(A-C) Steady-state transcript levels of *D. melanogaster* Toll pathway-regulated genes were measured by quantitative RT-PCR at different time points after a *M. luteus* challenge: *Drosomycin* (A), *Metchnikowin* (B), and *DIM1=BomS1*. These experiments are representative of three independent experiments. Gene expression was normalized against *rpl32* gene expression and the results are normalized to the expression at 48h with WT. No significant difference between WT and isogenic *BaraA* mutants was detected. (D) The cleavage of the prophenoloxidase was analyzed 4h after *M. luteus* septic injury by Western blotting using an anti-PPO1 antibody. This blot is representative of three out of four experiments.

Fig. 5 ***BaraA* plays a role in the host defense mediated by hemocytes against *E. faecalis* and *M. robertsii* through distinct processes**.

(A) Hemolymph was collected from adult *BaraA-mCherry* knock-in flies injected with *E. faecalis* for 12 hours or from untreated flies and the hemocytes were observed by fluorescence microscopy at 40X magnification. (B) Survival of *hmlGal4>UAS*-BaraA RNAi KD2 after an immune challenge with *E. faecalis*; one of two experiments yielding similar results. Statistical significance between wild type and KD flies, LogRank test ****P < 0.0001. (C) 4.6nl pHrodo-labeled *E. faecalis* were injected into flies, which were observed 30-45min post infection. (D) The quantification by ImageJ of the Phrodo fluorescent signal corresponding to bacteria present within an acidic compartment in hemocytes did not reveal any significant difference between WT and *BaraA* isogenized KO mutants. (E) Survival of *hmlGal4>UAS*-BaraA RNAi KD2 after an immune challenge with *M. robertsii* failed to reveal a significant difference of sensitivity to this infection with control *mCherry* RNAi flies; one out of two experiments. (F) Image of conidia stained by a polyclonal antibody raised against *M. robertsii* using a differential permeabilization procedure; conidia stained in yellow correspond to noningested conidia whereas green conidia (arrow) are found within plasmatocytes. (G) Phagocytosis index of the WT and *BaraA* larval hemocytes. 5000 *M. robertsii* conidia were injected into third-instar larvae, which were incubated for two hours 2 hours incubation at 29°C before being bled. The hemocytes were then processed as described above; 50 hemocytes were scored for each sample. ANOVA with Dunnett's post-hoc tests: **: p<0.01; ****: p< 0.0001.

Fig. 1

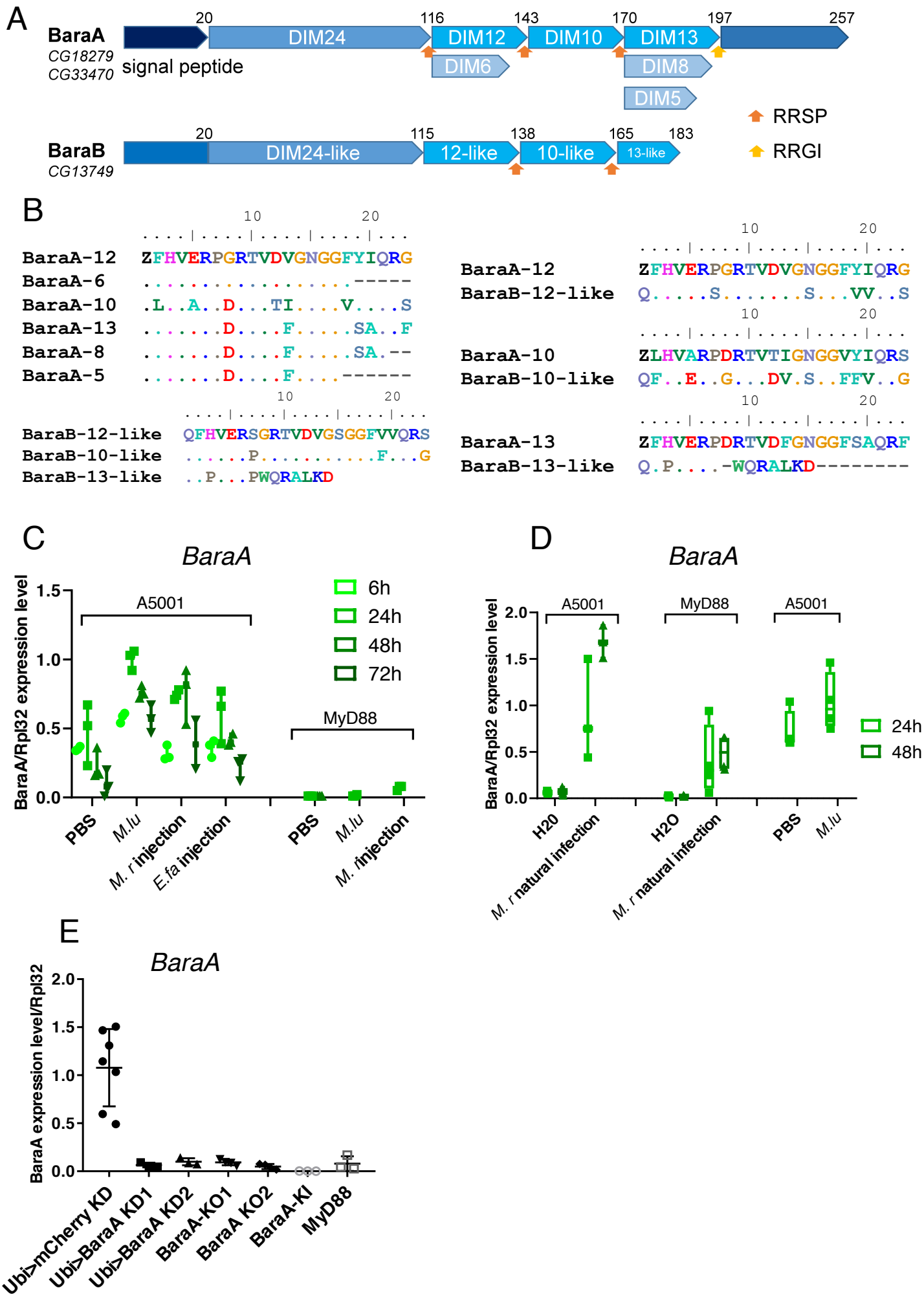
A
BaraA
CG18279
CG33470
signal peptide
20
DIM24
116
DIM12
143
DIM10
170
DIM13
197
257
DIM6
DIM8
DIM5
RRSP
RRGI
BaraB
CG13749
20
DIM24-like
115
12-like
138
10-like
165
13-like
183
B
BaraA-12 ZFHVERPGRTVDVGNGGFYIQRG
BaraA-6 .....-----
BaraA-10 .L..A..D...TI....V....S
BaraA-13 .....D....F.....SA..F
BaraA-8 .....D....F.....SA.--
BaraA-5 .....D....F....------
BaraB-12-like QFHVERSGRTVDVGSGGFVVQRS
BaraB-10-like .....P.....F...G
BaraB-13-like ..P...PWQRALKD
BaraA-12 ZFHVERPGRTVDVGNGGFYIQRG
BaraB-12-like Q.....S.....S...VV..S
BaraA-10 ZLHVARPDRTVTIGNGGVYIQRS
BaraB-10-like QF..E..G...DV.S..FFV..G
BaraA-13 ZFHVERPDRTVDFGNGGFSAQRF
BaraB-13-like Q.P....-WQRALKD--------
C
BaraA
BaraA/Rpl32 expression level
A5001
MyD88
6h
24h
48h
72h
PBS
M.lu
M. r injection
E.fa injection
D
BaraA
A5001
MyD88
A5001
24h
48h
H2O
M. r natural infection
E
BaraA
BaraA expression level/Rpl32
Ubi>mCherry KD
Ubi>BaraA KD1
Ubi>BaraA KD2
BaraA-KO1
BaraA KO2
BaraA-KI
MyD88

Fig. 2

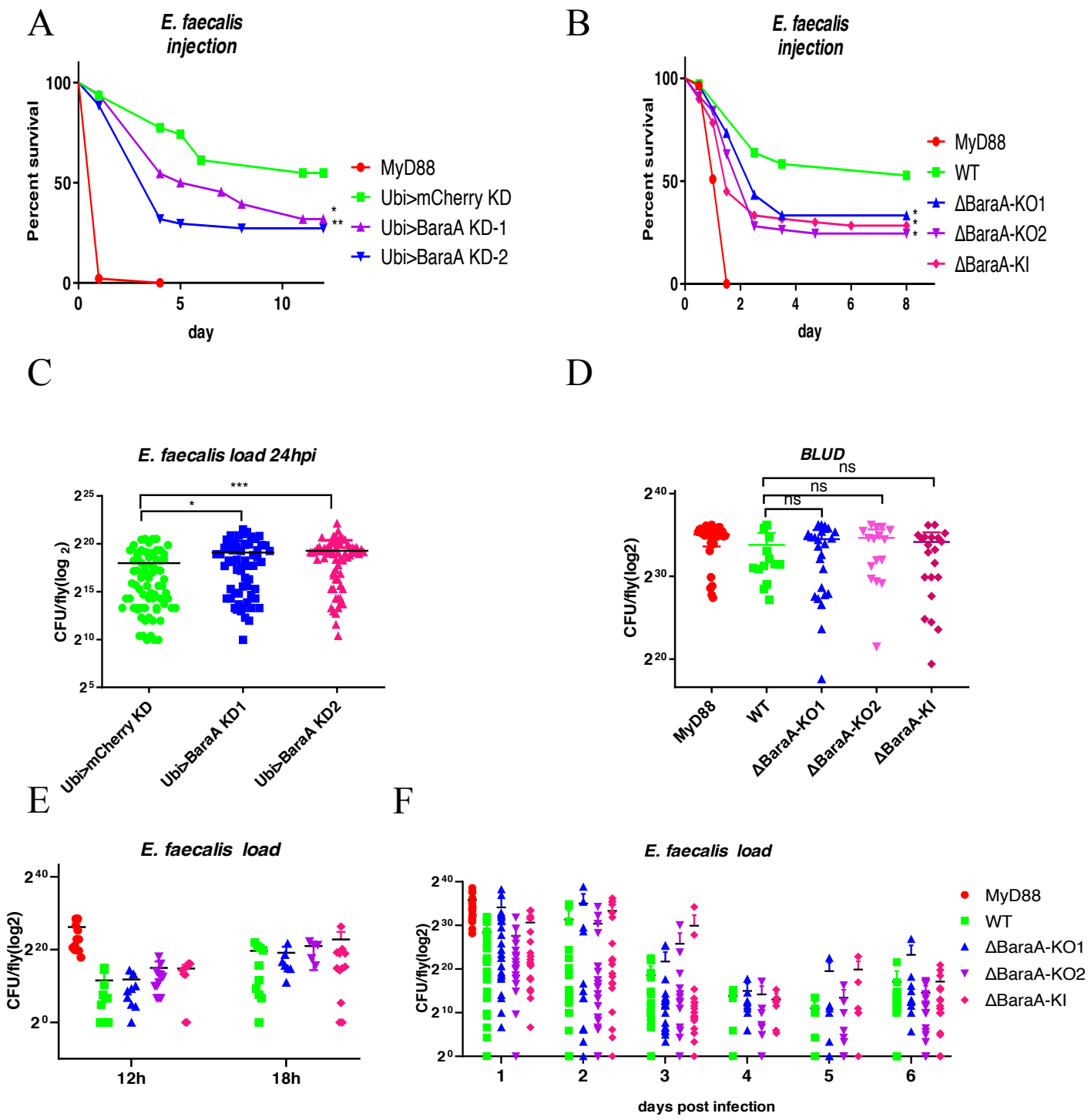
A
E. faecalis injection
Percent survival
day
MyD88
Ubi>mCherry KD
Ubi>BaraA KD-1
Ubi>BaraA KD-2
B
E. faecalis injection
Percent survival
day
MyD88
WT
ΔBaraA-KO1
ΔBaraA-KO2
ΔBaraA-KI
C
E. faecalis load 24hpi
CFU/fly(log 2)
Ubi>mCherry KD
Ubi>BaraA KD1
Ubi>BaraA KD2
D
BLUD
CFU/fly(log2)
ns
MyD88
WT
ΔBaraA-KO1
ΔBaraA-KO2
ΔBaraA-KI
E
E. faecalis load
CFU/fly(log2)
12h
18h
F
E. faecalis load
CFU/fly(log2)
days post infection
MyD88
WT
ΔBaraA-KO1
ΔBaraA-KO2
ΔBaraA-KI

Fig. 3

A

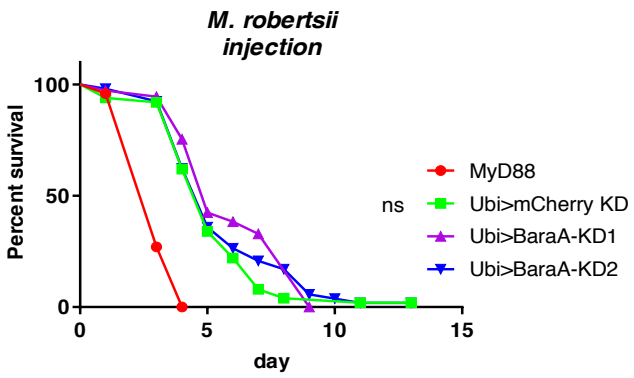
M. robertsii injection
Percent survival
100
50
0
0
5
10
15
day
ns
MyD88
Ubi>mCherry KD
Ubi>BaraA-KD1
Ubi>BaraA-KD2

B

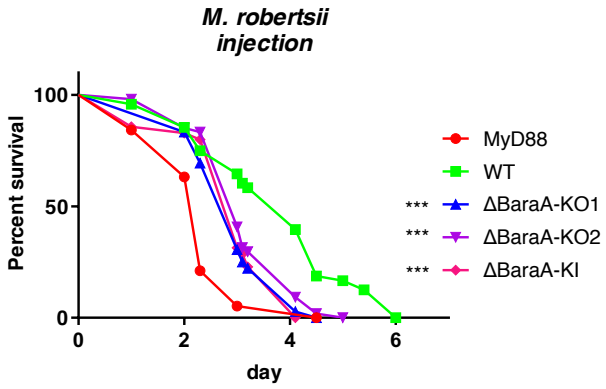
M. robertsii injection
Percent survival
100
50
0
0
2
4
6
day
MyD88
WT
*** ΔBaraA-KO1
*** ΔBaraA-KO2
*** ΔBaraA-KI

C

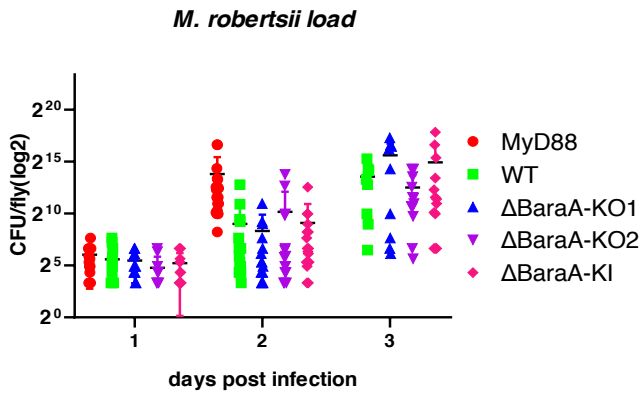
M. robertsii load
CFU/fly(log2)
2^{20}
2^{15}
2^{10}
2^{5}
2^{0}
1
2
3
days post infection
MyD88
WT
ΔBaraA-KO1
ΔBaraA-KO2
ΔBaraA-KI

D

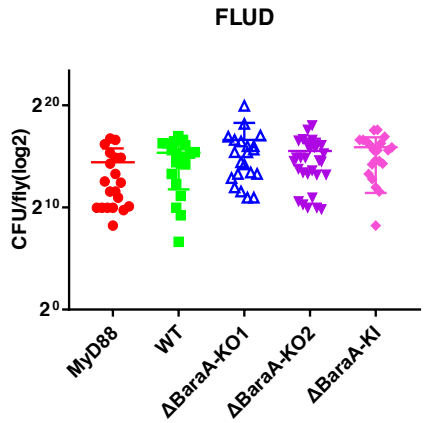
FLUD
CFU/fly(log2)
2^{20}
2^{10}
2^{0}
MyD88
WT
ΔBaraA-KO1
ΔBaraA-KO2
ΔBaraA-KI

Fig. 4

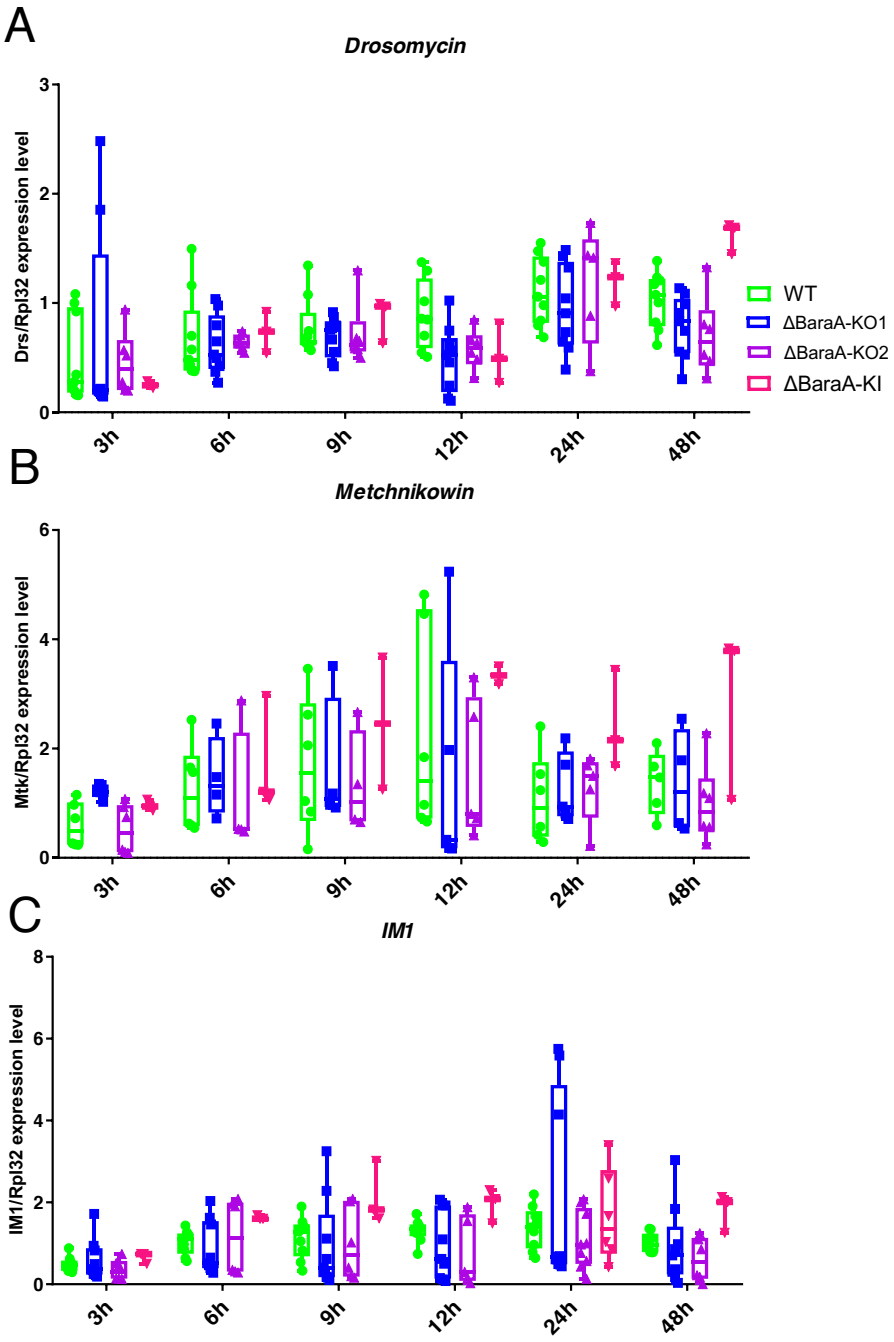
A
Drosomycin
Drs/Rpl32 expression level
0
1
2
3
3h
6h
9h
12h
24h
48h
WT
ΔBaraA-KO1
ΔBaraA-KO2
ΔBaraA-KI
B
Metchnikowin
Mtk/Rpl32 expression level
0
2
4
6
3h
6h
9h
12h
24h
48h
C
IM1
IM1/Rpl32 expression level
0
2
4
6
8
3h
6h
9h
12h
24h
48h

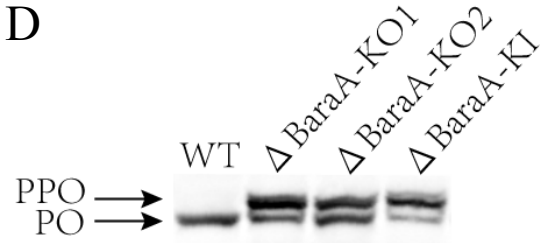
D
WT
Δ BaraA-KO1
Δ BaraA-KO2
Δ BaraA-KI
PPO
PO

Fig. 5

A

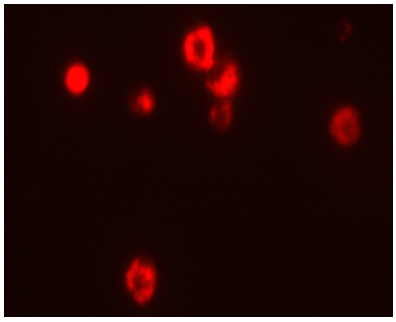

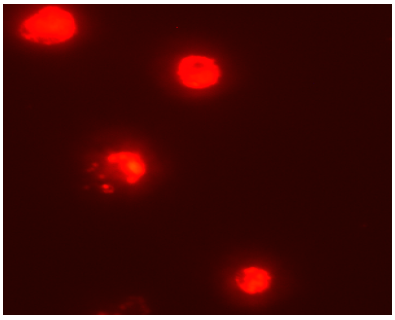

B

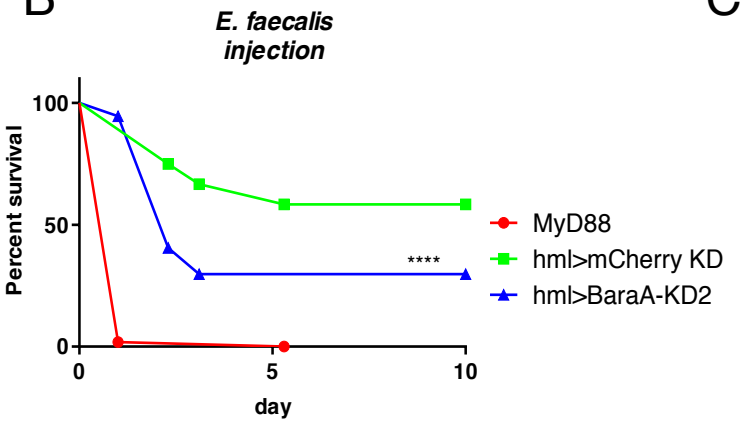

C

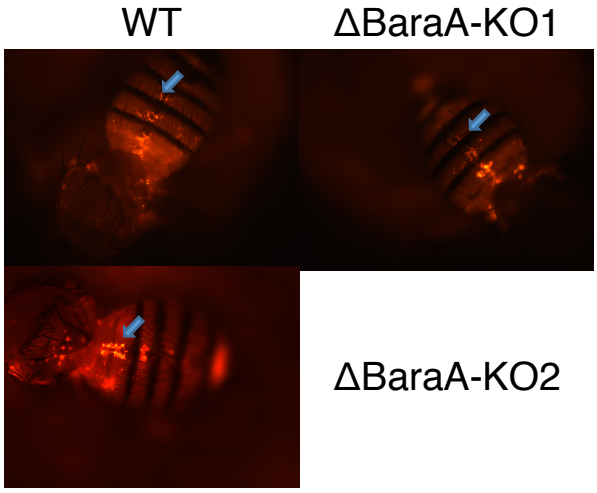

D

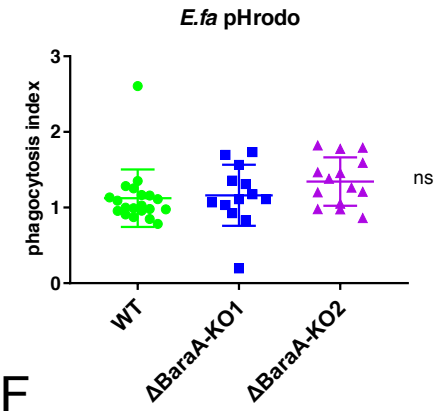

E

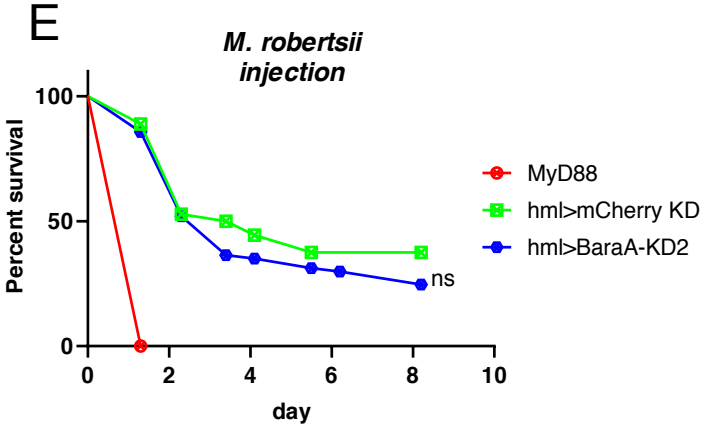

F

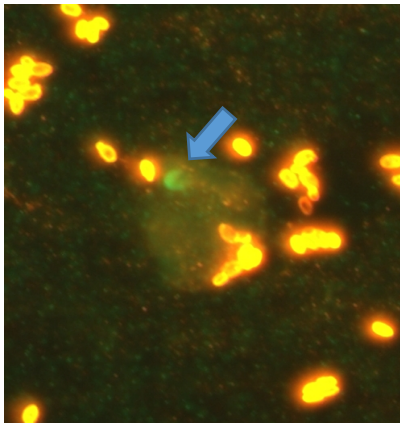
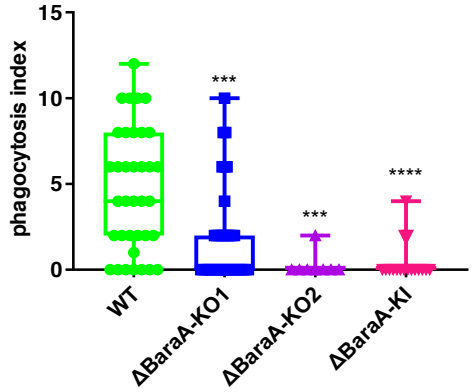
G